Atmospheric Environment 83 (2014) 80–89

Contents lists available at ScienceDirect

Atmospheric Environment

journal homepage: www.elsevier.com/locate/atmosenv

Observations of ammonia, nitric acid, and fine particles in a rural gas production region

Yi Li [a], Florian M. Schwandner [a,1], H. James Sewell [b], Angela Zivkovich [b], Mark Tigges [c], Suresh Raja [a,2], Stephen Holcomb [c,3], John V. Molenar [c], Lincoln Sherman [c], Cassie Archuleta [c], Taehyoung Lee [a,4], Jeffrey L. Collett Jr. [a,*]

[a] Department of Atmospheric Science, Colorado State University, Fort Collins, CO 80523, USA
[b] Shell Exploration and Production Co., Denver, CO 80237, USA
[c] Air Resource Specialists, Inc., Fort Collins, CO 80525, USA

HIGHLIGHTS

- Five years of measurements reveal low ammonia concentrations in western Wyoming.
- Ammonia and nitric acid concentrations show a strong seasonal variation.
- Ammonia concentrations peak in summer.
- Nitric acid concentrations peak in summer and winter.

ARTICLE INFO

Article history:
Received 7 April 2013
Received in revised form
26 September 2013
Accepted 2 October 2013

Keywords:
Ammonium
Nitrate
Gas/particle partitioning
Denuder
Wyoming

ABSTRACT

Continuous measurements of the atmospheric trace gases ammonia (NH_3) and nitric acid (HNO_3) and of fine particle ($PM_{2.5}$) ammonium (NH_4^+), nitrate (NO_3^-) and sulfate (SO_4^{2-}) were conducted using a denuder/filter system from December 2006 to December 2011 at Boulder, Wyoming, a region of active gas production. The average five year concentrations of NH_3, HNO_3, NH_4^+, NO_3^- and SO_4^{2-} were 0.17, 0.19, 0.26, 0.32, and 0.48 μg m^{-3}, respectively. Significant seasonal patterns were observed. The concentration of NH_3 was higher in the summer than in other seasons, consistent with increased NH_3 emissions and a shift in the ammonium nitrate (NH_4NO_3) equilibrium toward the gas phase at higher temperatures. High HNO_3 concentrations were observed both in the summer and the winter. Elevated wintertime HNO_3 production appeared to be due to active local photochemistry in a shallow boundary layer over a reflective, snow-covered surface. $PM_{2.5}$ NH_4^+ and SO_4^{2-} concentrations peaked in summer while NO_3^- concentrations peaked in winter. Cold winter temperatures drive the NH_3–HNO_3–NH_4NO_3 equilibrium toward particulate NH_4NO_3. A lack of NH_3, however, frequently results in substantial residual gas phase HNO_3 even under cold winter conditions.

© 2013 Elsevier Ltd. All rights reserved.

1. Introduction

Ammonia (NH_3) is the most abundant alkaline gas in the troposphere and is important for its ability to neutralize acidic components such as sulfuric acid (H_2SO_4) and nitric acid (HNO_3) which form, respectively, by oxidation of emissions of sulfur dioxide (SO_2) and nitrogen oxides (NO_x). NH_3 is also an important contributor to nitrogen deposition (Beem et al., 2010; Benedict et al., 2013), which can cause eutrophication, soil acidification and biotic community changes (Cowell and Apsimon, 1998; Groot Koerkamp et al., 1998). It is widely recognized that important sources of NH_3 include agricultural activities such as fertilization and livestock emissions (Li et al., 2006; Misselbrook et al., 2000; Sutton et al., 2000). Reactions of HNO_3 and H_2SO_4 with ambient NH_3 generally form submicron ammonium nitrate (NH_4NO_3) and ammoniated sulfate (NH_4HSO_4, $(NH_4)_2SO_4$, or other forms) particles which can adversely impact human respiratory health and

* Corresponding author.
E-mail address: collett@atmos.colostate.edu (J.L. Collett).
[1] Current address: Jet Propulsion Laboratory, California Institute of Technology, 4800 Oak Grove Drive, Pasadena, CA 91109, USA.
[2] Current address: Providence Engineering and Environmental Group, Irving, TX 75038, USA.
[3] Current address: NiSource, Merrillville, IN 46410, USA.
[4] Current address: Department of Environmental Science, Hankuk University of Foreign Studies, Yongin 449-791, Republic of Korea.

1352-2310/$ – see front matter © 2013 Elsevier Ltd. All rights reserved.
http://dx.doi.org/10.1016/j.atmosenv.2013.10.007

impair atmospheric visibility through visible light scattering. In the United States (U.S.) a set of Class 1 areas (including National Parks and Wilderness Areas) has been identified for protection from visibility impairment through the Regional Haze Rule. Because oil and gas production regions of the western U.S. are often located near these visibility-protected areas, close attention is paid to their emissions of fine particle precursors. In order to reduce NO_x emissions from natural gas drilling and production activities, for example, selective catalytic reduction (SCR) can be installed on drill rigs. While SCR can yield large reductions of NO_x emissions; however, there is a risk of increased NH_3 emission into the atmosphere.

Western Wyoming is one region of active recent gas development where several air quality concerns have been raised (McMurray et al., 2013). Emissions of NO_x have been of concern both because of possible impacts on regional haze and, especially, due to documented impacts on severe winter ozone episodes (Schnell et al., 2009). SCR implementation in the region has been active in recent years as one effort to limit winter ozone episodes. While these winter ozone episodes are believed to be local in nature, NO_x emission impacts on regional haze may be more widespread. Unfortunately, few measurements exist in the region of NH_3 and haze impact assessments are generally forced to rely on an assumed background NH_3 concentration level. While a number of recent studies have considered the role NH_3 plays in the formation of fine particles across the United States in both urban and rural areas (Bari et al., 2003; Benedict et al., 2013; Edgerton et al., 2007; Gong et al., 2011; Heald et al., 2012; Lee et al., 2008; Nowak et al., 2010; Sather et al., 2008), knowledge of atmospheric concentrations of NH_3, and their seasonal variability is still rather limited, especially in the interior western United States. Here we present five years of observations of concentrations of gaseous NH_3 and HNO_3 and fine particle concentrations of NH_4^+, SO_4^{2-} and NO_3^- from Boulder, Wyoming, a site in the heart of an active gas production region. These measurements provide the longest term record of NH_3 concentration measurements in this part of the U.S. and provide new insight into typical NH_3 concentrations in the region, their seasonal variability, and the gas-particle partitioning of the NH_3–NH_4^+–HNO_3–NO_3^-–SO_4^{2-} system that is one important contributor to regional haze.

2. Experimental methods

Measurements were made southwest of Boulder, Wyoming (42°43′7.9″N, 109°45′10.4″W) in the northwestern part of the Pinedale anticline area. Two visibility-protected areas, Bridger Wilderness Area and Fitzpatrick Wilderness Area, are located within 100 km. The Boulder area and nearby natural gas fields are situated on a high plateau between the Wind River Range to the east and the Wyoming Range to the west. Strong surface-based inversions, with inversion pools intersecting topography levels down to 50 m above ground (Schnell et al., 2009), are common in the region, especially during wintertime. The population density in Boulder, Wyoming is sparse with only 8.9 people per square km. The Jonah Gas Field and the Pinedale Anticline Gas Field, together representing one of the largest gas production regions in the U.S., are close to the sampling site with several active gas wells located approximately 3 km west of the sampling site. In 2008, there were more than 500 permitted wells in the Jonah Gas Field and an additional 3100 wells are expected to be drilled in this field over the next 75 years. Total production in this region in 2011 was nearly 171 billion cubic feet of natural gas and 1.5 million barrels of oil (http://www.encana.com/pdf/communities/usa/JonahField-FactSheet.pdf). NO_x from the gas extraction operations and transportation emissions are the largest contributor to local NO_x emissions (Fig. S1a). For NH_3 emissions, there are not many large sources in this immediate area. However, the Snake River Valley to the west of the measurement site is a large area of intense agricultural activity with elevated NH_3 emissions and concentrations (Clarisse et al., 2009) (Fig. S1b). Installation of more SCR systems in the Jonah-Pinedale region could elevate local NH_3 concentrations, contributing to more particle formation and visibility degradation.

Concentrations of gaseous NH_3 and HNO_3 and $PM_{2.5}$ (particles with an aerodynamic diameter less than 2.5 μm) inorganic ions (NH_4^+, SO_4^{2-}, NO_3^-, K^+, Mg^{2+} and Ca^{2+}) were sampled using a URG denuder/filter system (University Research Glassware, Inc., Model 3000CA), which was installed at 1.5 m height, followed by laboratory extraction and analysis by ion chromatography. The URG sampling system has been widely used because of its good performance in sampling acidic gaseous and volatile aerosols (Bari et al., 2003; Beem et al., 2010; Edgerton et al., 2007; Lee et al., 2004; Lin et al., 2006). Air was drawn through a Teflon-coated $PM_{2.5}$ cyclone followed by two 242 mm annular denuders connected in series, a 47-mm filter pack containing a nylon filter (Nylasorb, pore size1μm, Pall Corporation) and another annular denuder (from Dec. 2006 through July 11th 2008, samples were collected used a backup coated filter rather than a 3rd denuder). Air flow was maintained at a constant mass flow rate by means of a mass flow controlled pump (URG Inc.). The total flow rate through the system was nominally 10 L min^{-1} at ambient conditions. Actual sample volumes were determined using a sample pressure-compensated dry gas meter. The first denuder was coated with sodium chloride (NaCl) to collect gaseous HNO_3 and the second was coated with phosphorus acid (H_3PO_4) to collect gaseous NH_3. The last denuder (or coated filter) was phosphorus acid-coated to collect any NH_3 re-volatilized from NH_4^+ salt particles collected on the filter. Nylon filters have been shown to retain volatilized HNO_3, but loss of NH_4^+ can be significant (Yu et al., 2006). The sample trains were prepared in the lab at Colorado State University (CSU), and then shipped weekly and installed by a local site operator. Samples were typically collected twice a week (one 4 day sample and one 3 day sample). After sampling, the sample train was shipped back to the lab at CSU. The denuders were extracted with 10 ml deionized water, and the extracts refrigerated before analysis. Nylon filters were ultrasonically extracted for 55 min in 6 ml of high purity deionized water. Ion chromatography using a Dionex dual channel system was used to analyze the denuder and filter extracts. Cations (Na^+, NH_4^+, K^+, Mg^{2+} and Ca^{2+}) in the samples were separated with a methanesulfonic acid eluent on a Dionex CG12A guard column and CS12A separation column followed by a CSRS ULTRA II suppressor and detected by a Dionex conductivity detector. Anions (Cl^-, NO_3^-, SO_4^{2-}) in the samples were separated with a carbonate/bicarbonate eluent on a Dionex AG14A guard column and AS14A separation column followed by an ASRS ULTRA II suppressor and detected using a Dionex conductivity detector.

Meteorological data, including temperature, relative humidity and wind speed, were obtained from a co-located weather station (2 m height) operated by Air Resource Specialists, Inc.

Sample recovery was high, although there were occasional periods where samples could not be collected on the normal schedule (e.g., from bad weather affecting sampler shipment or operator access). Field and laboratory blanks were collected throughout the study and used to determine the method detection limit (MDL) and to blank-correct results. The MDLs for NH_3, HNO_3, NH_4^+, SO_4^{2-}, NO_3^-, K^+, Mg^{2+} and Ca^{2+} were determined as 0.012, 0.012, 0.002, 0.017, 0.001, 0.005, 0.007 and 0.023 μg m^{-3}, respectively. Replicate extract analyses yielded measurement precisions of 5.4%, 3. 8%, 3.5%, 0.8%, 2.1%, 4.9%, 7.6%, and 6.2% (relative standard deviation) for NH_3, HNO_3, NH_4^+, SO_4^{2-}, NO_3^-, K^+, Mg^{2+} and Ca^{2+}, respectively.

3. Results and discussion

From December 2006 through December 2011, 505 samples were collected. The summary of the annual and seasonal mean and standard deviation for all the trace gas concentrations, particulate species concentrations and meteorological parameter values are summarized in Table S1 in the supplement. Because of the high latitude of this continental sampling site and the monthly average temperatures, the following months were defined as representing specific seasons, for the purpose of discussing the analytical results below: April and May were defined as spring; June, July and August as summer; September and October as fall; and November through March as winter.

Fig. 1 shows time series of the concentrations of gaseous NH_3 and HNO_3 and $PM_{2.5}$ NH_4^+ and NO_3^- across the five year measurement period. NH_3 concentrations peak in summer while NO_3^- concentrations peak in winter. HNO_3 exhibits a distinct bimodal seasonal concentration pattern with summer and winter maxima. As shown in Fig. 2, NH_4^+, SO_4^{2-} and NO_3^- were the three most abundant inorganic ions in $PM_{2.5}$ in all seasons. The concentration of NH_4^+ varied least across seasons. During the warm season SO_4^{2-} was the most abundant inorganic anion in $PM_{2.5}$, while during winter the concentration of NO_3^- was highest. More details concerning the trends of each of the trace gas and particulate species will be presented below.

3.1. Concentrations of major gas and fine particle species, their seasonal patterns, and gas-particle partitioning

Gaseous NH_3 exhibited a clear seasonal concentration pattern, ranging from an average concentration of 0.04 μg m^{-3} in winter to 0.39 μg m^{-3} in summer (Fig. 3a). The maximum quarterly NH_3 average concentration was 0.47 μg m^{-3} in summer 2008, 15 times higher than the winter 2008–2009 average of 0.03 μg m^{-3}. The significantly higher summer concentration reflects a strong influence of temperature. Previous studies have reported similar phenomena (Edgerton et al., 2007; Gupta et al., 2003; Meng et al., 2011; Plessow et al., 2005; Walker et al., 2004). Higher levels of NH_3 in the summer are consistent with the positive influence of higher temperatures on NH_3 emissions (e.g., from natural soils, agricultural operations, and fires) and the decomposition of particulate NH_4NO_3 into gaseous NH_3 and HNO_3.

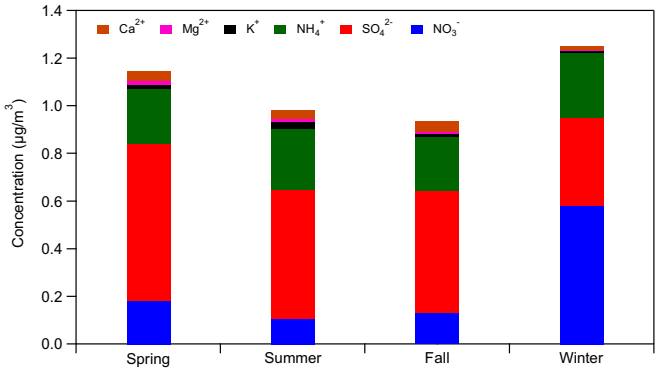

Fig. 2. Average mass concentrations of the chemical species in $PM_{2.5}$ by season across the 5 year sampling period.

One potential local source of NH_3 is increased use of SCR for high-efficiency NO_x control on drill rigs in the region. While use of SCR increased during the period of observation at Boulder, however, there is no clear increase in local NH_3 concentrations over the study. The annual mean concentration of NH_3 did not significantly increase during the study period. From 2007 to 2011, the annual NH_3 average concentrations in each year were 0.14, 0.20, 0.23, 0.15 and 0.13 μg m^{-3}, respectively, suggesting that SCR emissions did not noticeably influence local concentrations of ambient NH_3.

Table S2 shows cross-correlation coefficients for measured trace gases, particle ions and meteorological parameters. Some

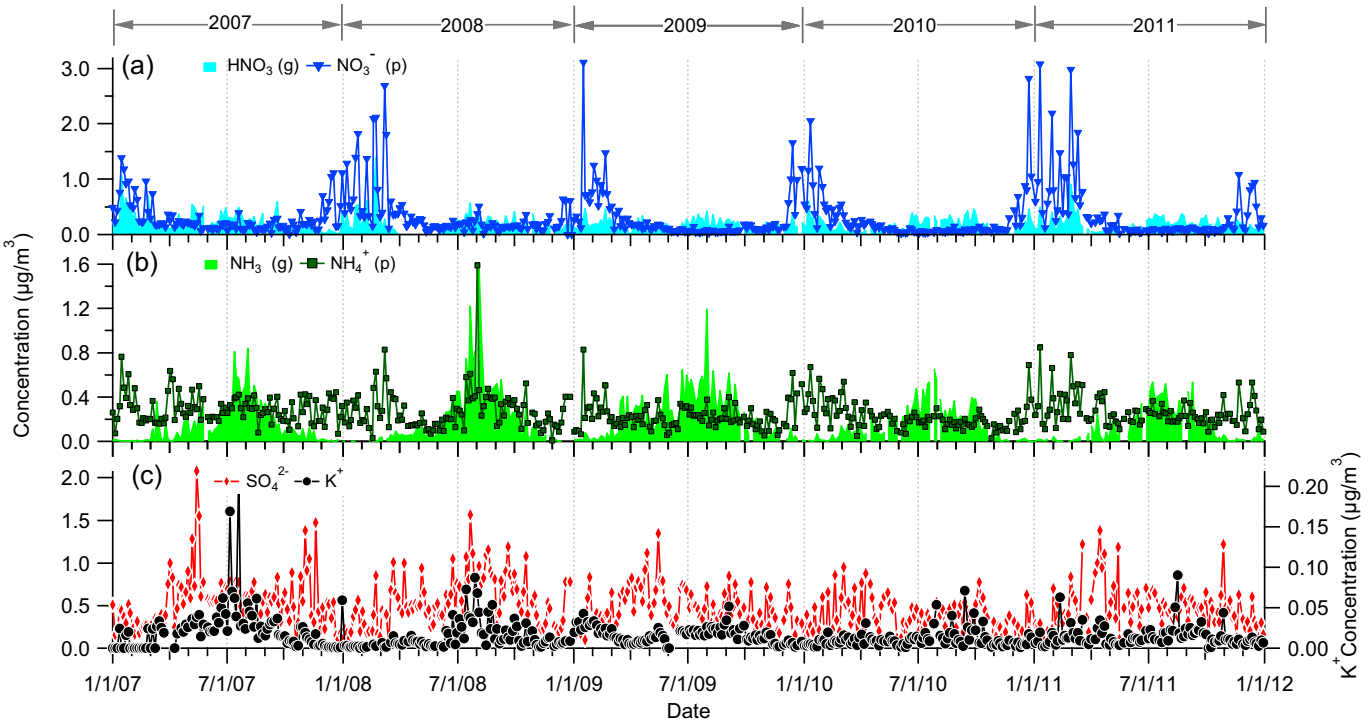

Fig. 1. Temporal variations of concentrations of (a) HNO_3 and NO_3^-, (b) NH_3 and NH_4^+ and (c) SO_4^{2-} and K^+ from 2007 through 2011 at Boulder, Wyoming.

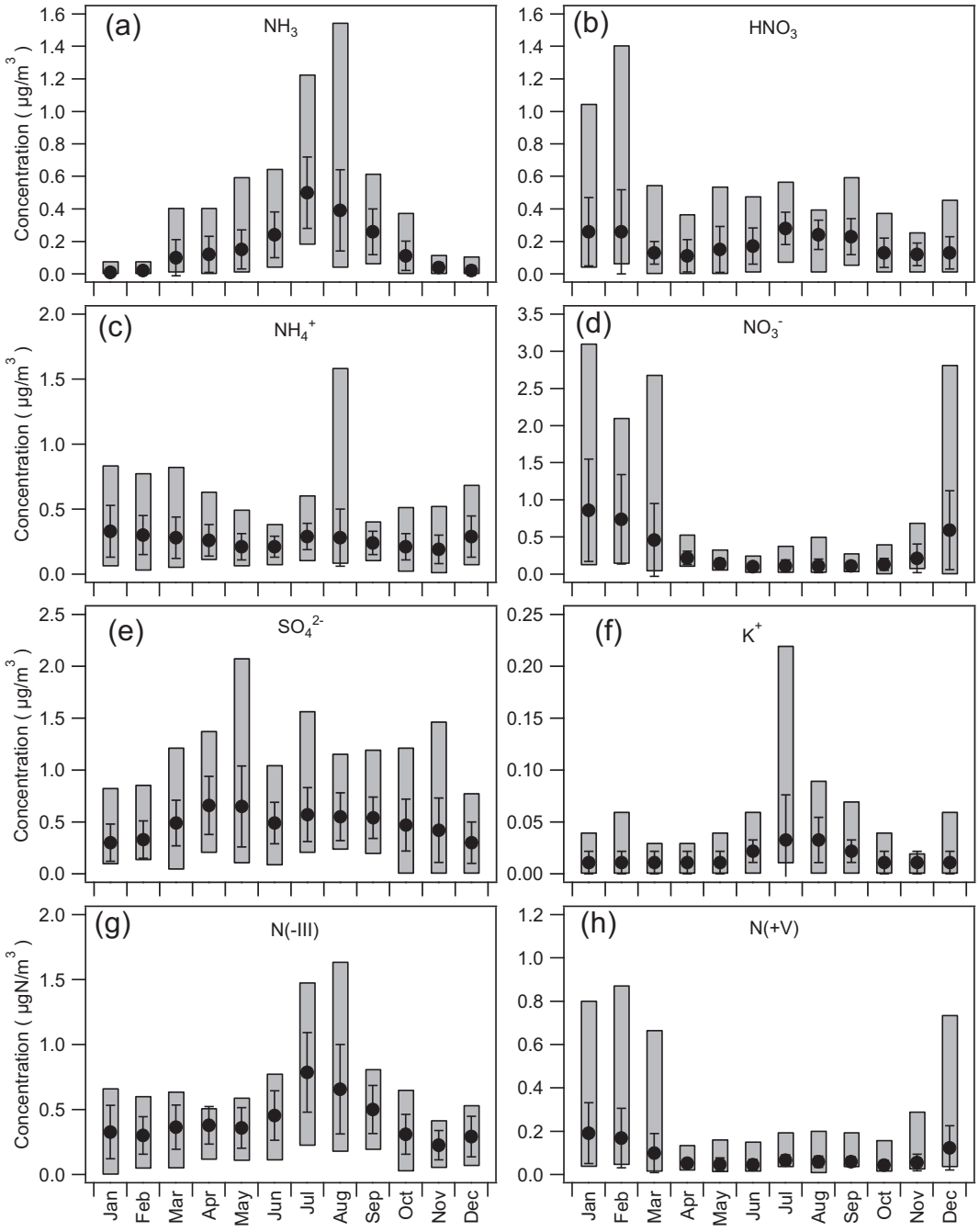

Fig. 3. The monthly variation of (a) NH_3, (b) HNO_3, (c) NH_4^+, (d) NO_3^-, (e) SO_4^{2-}, (f) K^+, (g) N(-III) and (h) N(+V) concentrations from 2007 to 2011. The gray shading represents minimum and maximum concentrations and the y-error bars represent standard deviations of average concentrations. For panels (a) to (f) the concentrations are expressed in μg m^{-3}; in panels (g) and (h) the concentrations are expressed as μgN/m^3.

correlation was found between NH_3 and K^+ ($r^2 = 0.16$). As illustrated by satellite fire-detect images (Fig. S2), there were more wild fires present around Boulder, Wyoming in 2007 and 2008; the correlation coefficients (r^2) between NH_3 and K^+ in those two years were 0.33 and 0.40. As a marker of biomass burning, the correlation between NH_3 and K^+ may suggest a positive influence of fire emissions on NH_3 concentrations (Anderson et al., 2003; Hegg et al., 1988; McMeeking et al., 2009; Sutton et al., 1995).

A background NH_3 mixing ratio of 1 ppbv is often assumed when estimating impacts of NO_x emissions on visibility and regional haze in western regions of the U.S. where ambient NH_3 concentration data are sparse or unavailable. Such estimates might be made, for example, through plume dispersion simulations using CALPUFF or other EPA-preferred models. The 5-year Boulder data records provide a better basis for choosing a representative background NH_3 concentration for the Pinedale region. Fig. 4 reveals that seasonal mean NH_3 mixing ratios ranged between a maximum of 0.85 ppbv (in summer 2008) and 0.03 ppbv (in winter 2010). The average for the full 5-year study period was 0.30 ppbv, less than one-third of the typically assumed background level. Even if $PM_{2.5}$ NH_4^+ (much of which certainly reacted with sulfuric and nitric acids upwind of the measurement region) and gaseous NH_3 are combined, the average mixing ratio (0.63 ppbv) remains well below 1 ppbv. Assumption of a 1 ppbv NH_3 background concentration in

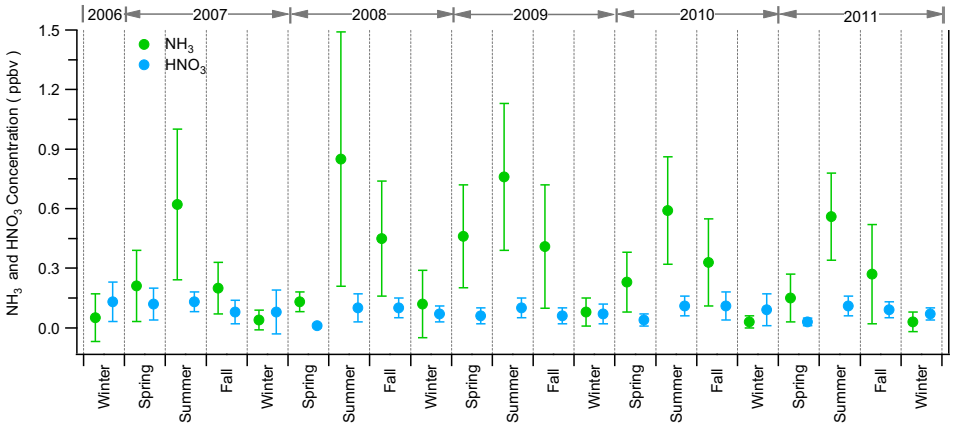

Fig. 4. The seasonal variations of NH_3 and HNO_3 mixing ratios from 2007 to 2011. The plotted points are the seasonal mean values and the Y-error bars represent standard deviations.

model simulations, therefore, will lead to an overprediction of visibility impacts associated with local NO_x emissions.

The five year average HNO_3 mixing ratio was observed to be 0.03 ppbv, indicating typically low concentrations of HNO_3 occur in this area. Seasonal mean HNO_3 mixing ratios (Fig. 4) ranged between 0.13 ppbv (in summer 2007) and 0.01 ppbv (in spring 2008). As illustrated in Fig. 3b, HNO_3 concentrations display a distinct bimodal seasonal pattern, with higher average concentrations in the summer (0.23 μg m^{-3}) and in mid-winter (January/February average = 0.26 μg m^{-3}) than in other seasons. One also can see in Fig. 4 that variability in observed HNO_3 concentrations is quite high in January and February. Previous studies have generally shown that HNO_3 peaks in summer with lower concentrations during winter (Adon et al., 2010; Gupta et al., 2003; Lee et al., 1999; Plessow et al., 2005). Increased concentrations of HNO_3 are expected in the summer because of more intense and longer lasting photochemical activity associated with higher sun angles and longer days. Higher summer temperatures also promote dissociation of NH_4NO_3 back to gaseous NH_3 and HNO_3, as discussed above (Seinfeld and Pandis, 2006). The high winter concentrations observed at Boulder, by contrast, are quite unusual. The peak wintertime HNO_3 concentration climbed as high as 1.40 μg m^{-3} for a single sample collected from February 22nd–25th in 2008. A closer look at the HNO_3 timeline in Fig. 1 reveals frequent winter periods of elevated HNO_3 concentrations. Other measurements at Boulder reveal that this area is frequently subject to periods of elevated winter ozone (Schnell et al., 2009) that occur during sunny winter periods when snow covers the ground. Strong nocturnal and morning temperature inversions that set up under these conditions trap local emissions of NO_x and volatile organic compounds, associated largely with local energy production activities, in a shallow mixing layer while daytime photochemical activity is enhanced by strong reflectance from the bright snow surface. The photochemical reactions that generate ozone concentrations well in excess of the U.S. National Ambient Air Quality Standard can also lead to substantial oxidation of the locally emitted NO_X to HNO_3. While cold winter conditions favor reaction of HNO_3 with NH_3 to form fine particle NH_4NO_3 (as evidenced by the winter NH_4NO_3 spikes in Fig. 1), the Boulder observations reveal that all gaseous NH_3 has often been consumed during these episodes leaving a substantial fraction of the HNO_3 "trapped" in the gas phase.

Ambient NH_4^+ concentrations at Boulder exhibited little seasonal pattern (Fig. 3c). The annual mean concentrations for 2007 to 2011 were also similar to each other at 0.29, 0.28, 0.23, 0.22 and 0.27 μg m^{-3}, respectively. Formation of fine particle NH_4^+ is influenced by a variety of factors, including the availability of gaseous NH_3 and the availability of acidic sulfate aerosol and gaseous HNO_3. Increases in NH_3 and SO_4^{2-} at Boulder during warmer months of the year will tend to increase NH_4^+ concentrations as well. Formation of fine particle NH_4NO_3, however, is favored in winter. As previously discussed, the formation of NH_4NO_3 is thermodynamically favored by high relative humidity and low temperatures. During the winter in Boulder, the average temperature was −7.8 °C and average relative humidity was 72.5%. These offsetting seasonal patterns appear to result in an overall NH_4^+ concentration pattern that shows little seasonality at Boulder.

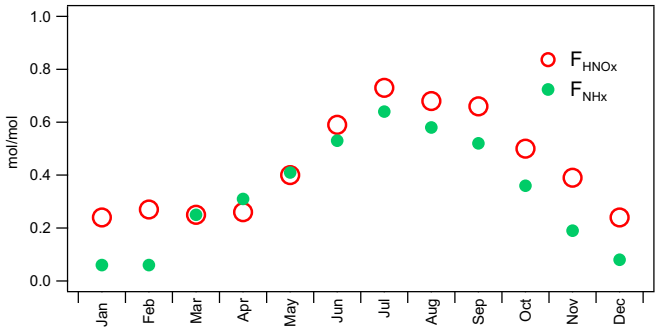

Fig. 5. Monthly variation of the ammonia conversion ratio (F_{NH_3}) and nitric acid conversion ratio (F_{HNO_3}). See text for details.

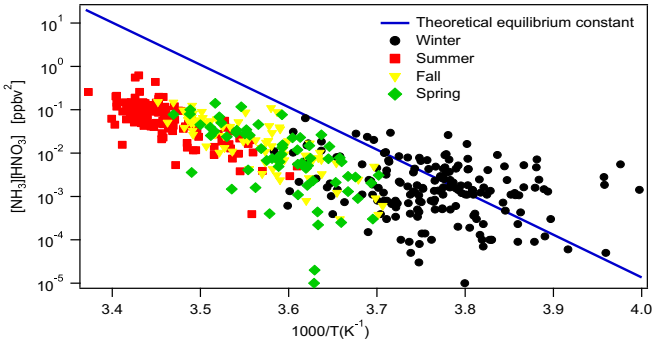

Fig. 6. Comparison of the measured [NH_3 (gas)][HNO_3(gas)] product with the theoretical equilibrium constant for NH_4NO_3 as a function of temperature across the different seasons.

The annual average concentrations of $PM_{2.5}$ NO_3^- measured at Boulder were 0.30, 0.36, 0.29, 0.27 and 0.37 μg m^{-3} in 2007 through 2011, respectively. The NO_3^- concentrations exhibited a strong seasonality, with maximum values in winter and minimum values in summer (Fig. 3d). Because NH_4NO_3 formation is not favored under the warm, dry conditions of summer, the mean summer NO_3^- concentration was only 0.11 μg m^{-3}. In winter, it increased to 0.60 μg m^{-3}, as NH_4NO_3 formation was more strongly favored. As indicated in Fig. 3d, considerable variability was also observed in winter NO_3^- concentrations, similar to the pattern discussed above for HNO_3, with maximum observed concentrations exceeding 2.0 μg m^{-3} in December, January, February, and March.

SO_4^{2-} shows a seasonal cycle with maximum values in the warm season (Fig. 3e). This seasonal pattern is typical of SO_4^{2-}, due to enhanced photochemical activity and higher concentrations of hydroxyl radical, which can oxidize SO_2 to SO_4^{2-} (Behera and Sharma, 2010). In-cloud oxidation of SO_2 to SO_4^{2-} can also be enhanced in summer when hydrogen peroxide concentrations are typically higher. Annual average concentrations of SO_4^{2-} at Boulder in 2007 through 2011 were 0.54, 0.53, 0.47, 0.38, and 0.47 μg m^{-3}.

In addition to anthropogenic emissions of nitrogen and sulfur species, wild and prescribed fires also contribute significantly to fine particle concentrations in the western U.S. (Jaffe et al., 2008; Malm et al., 2004). Water soluble potassium ion concentrations, one marker of biomass burning (Andreae, 1983; Duan et al., 2004), were elevated in summer (Fig. 3f). The average concentration of K^+ in the summer was 0.03 μg m^{-3}, which was nearly three times higher than the value in the winter (See Table S1). Not surprisingly, summer K^+ concentrations varied substantially; interannual variability in fire occurrence and the influence of emissions from fires that do occur on air quality at Boulder are expected. Across the sampling period, a number of wild fires occurred upwind of the site in summer.

Given the seasonally varying partitioning of NH_3/NH_4^+ and HNO_3/NO_3^- between the gas and particle phases, it is useful to also examine seasonal changes in total reduced inorganic nitrogen in the −3 oxidation state [N(-III) = NH_3 + NH_4^+] and in total oxidized inorganic nitrogen in the +5 oxidation state [N(+V) = HNO_3+NO_3^-]. As illustrated in Fig. 3g, N(-III) concentrations show a peak in the summer months, consistent with higher NH_3 emissions and greater SO_4^{2-} concentrations at this time of year. N(+V) concentrations, by contrast, peak in the winter months. This winter peak reflects the formation of HNO_3 in a shallow boundary layer during winter ozone episodes as well as winter formation of fine particle NH_4NO_3, with its longer atmospheric residence time than HNO_3.

To investigate the seasonal phase changes of NH_3/NH_4^+ and HNO_3/NO_3^-, we define *the ammonia gas fraction* (F_{HN_3} = the NH_3 gas concentration divided by the sum of the NH_3 gas and fine particle NH_4^+ concentrations) and *the nitric acid gas fraction* (F_{HNO_3} = the HNO_3 gas concentration divided by the sum of the HNO_3 gas and fine particle NO_3^- concentrations), where all concentrations are expressed in molar units. The monthly average partitioning for the reduced and oxidized inorganic nitrogen forms is plotted in Fig. 5. There was a gradual transition from the cooler months, when the particle phase was favored, to the warmer months, when the gas phase was favored, for both species. A maximum monthly average

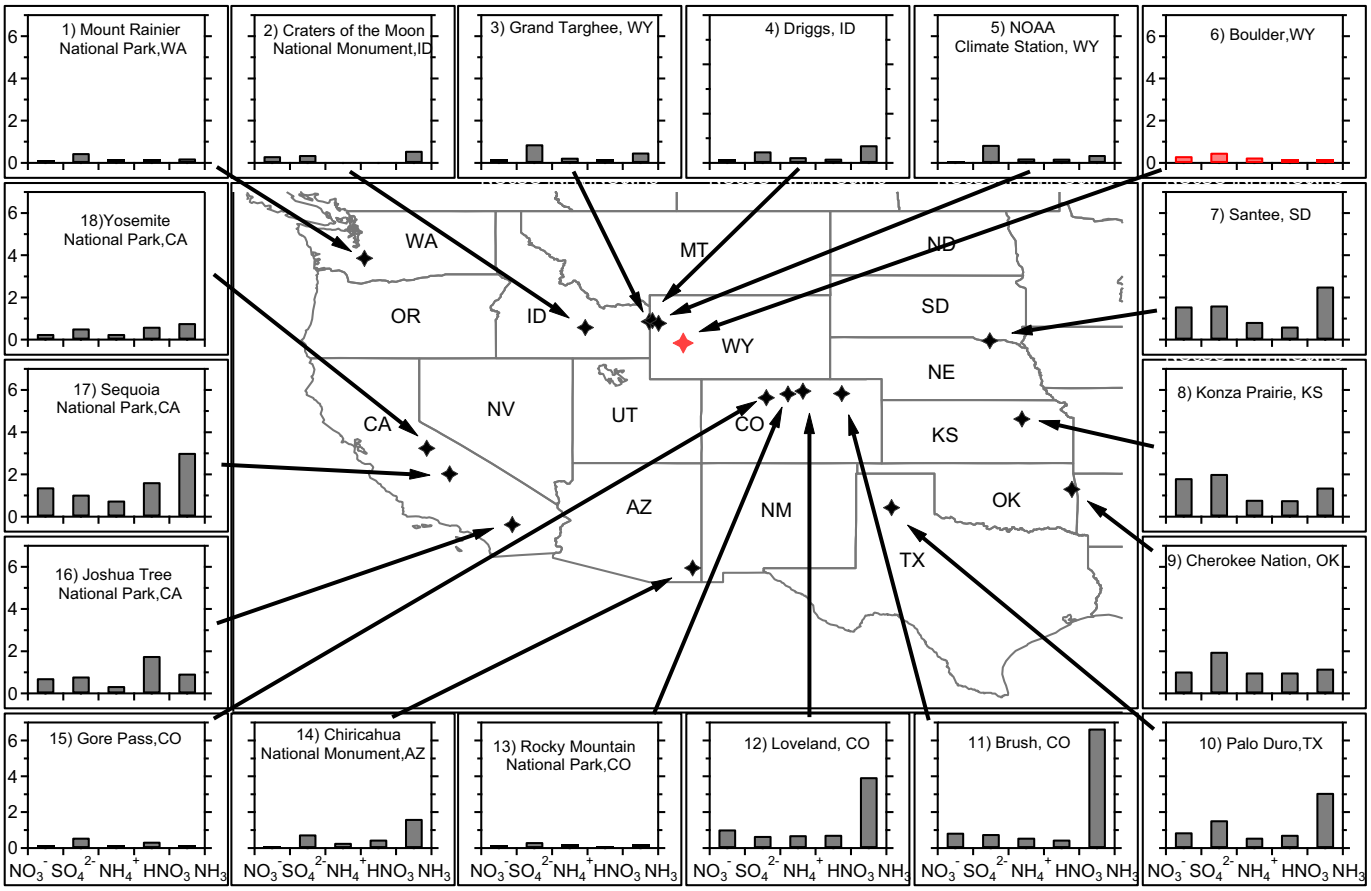

Fig. 7. Comparison of average levels of gases and aerosol species concentrations for this study and other sampling locations in the western U.S. There was no measurement of NH_4^+ and HNO_3 at Craters of the Moon National Monument, Idaho. Concentrations are in μg m^{-3}. More information about the comparison data can be found in Table S3.

in the gas phase fraction of NH_3 occurred in July (0.64). This was more than 10 times higher than the minimum monthly average of 0.06 which occurred in January. Similarly, the HNO_3 gas fraction (F_{HNO_3}) was found to be highest in summer (0.73 in July) and lowest in winter (0.24 in January). The high summer level of F_{HN_3} reflects greater NH_3 emissions and the thermodynamic tendency for NH_4NO_3 to dissociate to NH_3 and HNO_3 at high temperature. The higher summer value of F_{HNO_3} also reflects the tendency for NH_4NO_3 to dissociate at higher temperatures. The still appreciable winter F_{HNO_3} level, which is not typical of previous results (Bari et al., 2003; Gupta et al., 2003; Sharma et al., 2007), reflects the continued photochemical production of HNO_3 at levels which exceed the amount of NH_3 available to participate in NH_4NO_3 formation.

Shifts in the equilibrium partitioning among gaseous NH_3 and HNO_3 and particulate NH_4NO_3 depend on relative humidity (RH), temperature (T) and the concentrations of NH_3 and HNO_3. Ambient relative humidity at the Boulder measurement site was usually less than the deliquescence relative humidity (DRH) of NH_4NO_3 so that we can simplify matters and consider here formation of solid NH_4NO_3. Under this condition, this reaction's equilibrium constant (K_p) is the expected product of the NH_3 and HNO_3 concentrations and is given by the empirical formula (R1):

$$\ln K_p = 84.6 - \frac{24200}{T} - 6.1 \times \ln\frac{T}{298} \quad (1)$$

where K_p is in units of ppbv^2 and T is measured ambient temperature in Kelvin (Stelson and Seinfeld, 2007). The measured, apparent reaction constant (K_m) can be described as follows (R2):

$$K_m = [NH_3] \times [HNO_3] \quad (2)$$

where $[NH_3]$ is the gaseous NH_3 mixing ratio (ppbv) and $[HNO_3]$ is the gaseous HNO_3 mixing ratio (ppbv). NH_4NO_3 formation is favored when K_m exceeds K_p. Fig. 6 shows the variation of both the theoretical equilibrium constant (shown as a solid line) and measured constant values (for each sample) with temperature ($1000/T$) across all seasons. This presentation of the data clearly illustrates that NH_4NO_3 formation is only favored during wintertime; even then, it is not favored during all sample periods. At warmer times of the year, the product of NH_3 and HNO_3 concentrations is insufficient to yield NH_4NO_3 formation at seasonal temperatures.

3.2. Comparison with other measurements

Fig. 7 presents a comparison of observations from this study with other observations from the Clean Air Status and Trends Network (CASTNET; http://www.epa.gov/castnet/), the Interagency Monitoring of Protected Visual Environments (IMPROVE; http://vista.cira.colostate.edu/improve), the National Atmospheric Deposition Program Ammonia Monitoring Network (AMoN; http://nadp.sws.uiuc.edu/amon/) and seven sets of ambient composition measurements completed by our lab at CSU in the western U.S. (Table S3). Concentrations of particle and gas phase species observed at Boulder were, overall, among the lower average concentrations measured across this set of western sites. Comparing mean values of NH_3 and HNO_3 and fine particle NH_4^+, NO_3^-, and SO_4^{2-} at Boulder with the other rural locations, the concentrations

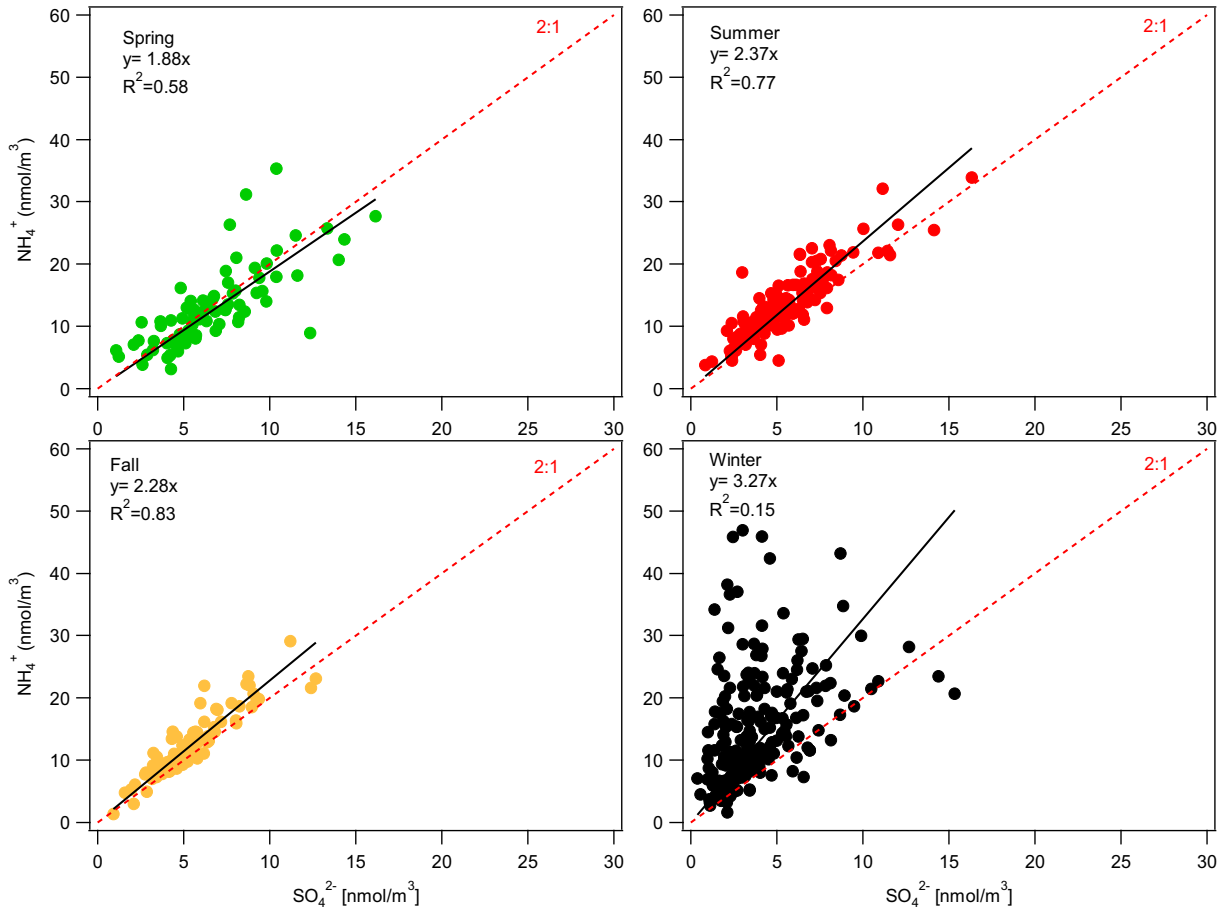

Fig. 8. Seasonal relationships of NH_4^+ versus SO_4^{2-} concentrations.

measured at Boulder were generally lower than those observed at sites further east such as Santee Sioux, South Dakota, Konza Prairie, Kansas, Cherokee Nation, Oklahoma, and Palo Duro, Texas. They were also significantly lower than concentrations measured closer to more populated areas, such as those at Sequoia National Park, California, Joshua Tree National Park, California, and Loveland, Colorado. Boulder, Wyoming NH_3 concentrations were substantially lower than NH_3 concentrations measured at sites more strongly impacted by regional agriculture/animal feeding operations, such as Brush, Colorado. Overall concentrations were fairly similar, however, between Boulder and other remote sites in central and western Colorado and in western Wyoming, suggesting some regional representativeness of the concentrations measured in Boulder (aside from the winter ozone episodes). Although the Boulder measurement site is only approximately 65 km from the Snake River Plain Valley, an area of intense agricultural activity with high NH_3 emissions (Clarisse et al., 2009), the low NH_3 concentrations observed at Boulder suggest that the Wyoming (Palisades) Mountain Range blocks at least the most direct transport of these emissions while other local NH_3 emissions are limited in their contributions to ambient NH_3 concentrations.

3.3. Interspecies correlations, the measured ion charge balance, and the importance of organic acids

Fig. 8 illustrates the correlation between fine particle NH_4^+ and SO_4^{2-} in different seasons. Significant correlations were found in all seasons except in winter. The highest correlation ($r^2 = 0.84$) was in the fall and the lowest was in the winter ($r^2 = 0.15$). The weak correlation in winter results from substantial NH_4NO_3 formation during this time period. If one plots the excess NH_4^+ (the amount beyond that needed to fully neutralize fine particle SO_4^{2-}), one finds it to be strongly correlated with fine particle NO_3^- during winter ($r^2 = 0.76$; slope of 0.81), modestly correlated in fall ($r^2 = 0.31$; slope of 1.01), and showing almost no correlation in spring and summer (see Fig. S3).

Overall, on the basis of the seasonal variation of comparisons between NH_4^+ and SO_4^{2-} and excess NH_4^+ and NO_3^-, one can conclude that most fine particle NH_4^+ in summer exists as $(NH_4)_2SO_4$ while both $(NH_4)_2SO_4$ and NH_4NO_3 are found in fine particles in winter. An excess of NH_4^+ in summer when NO_3^- concentrations are low, however, suggests that other unmeasured anionic species might also be important components of the

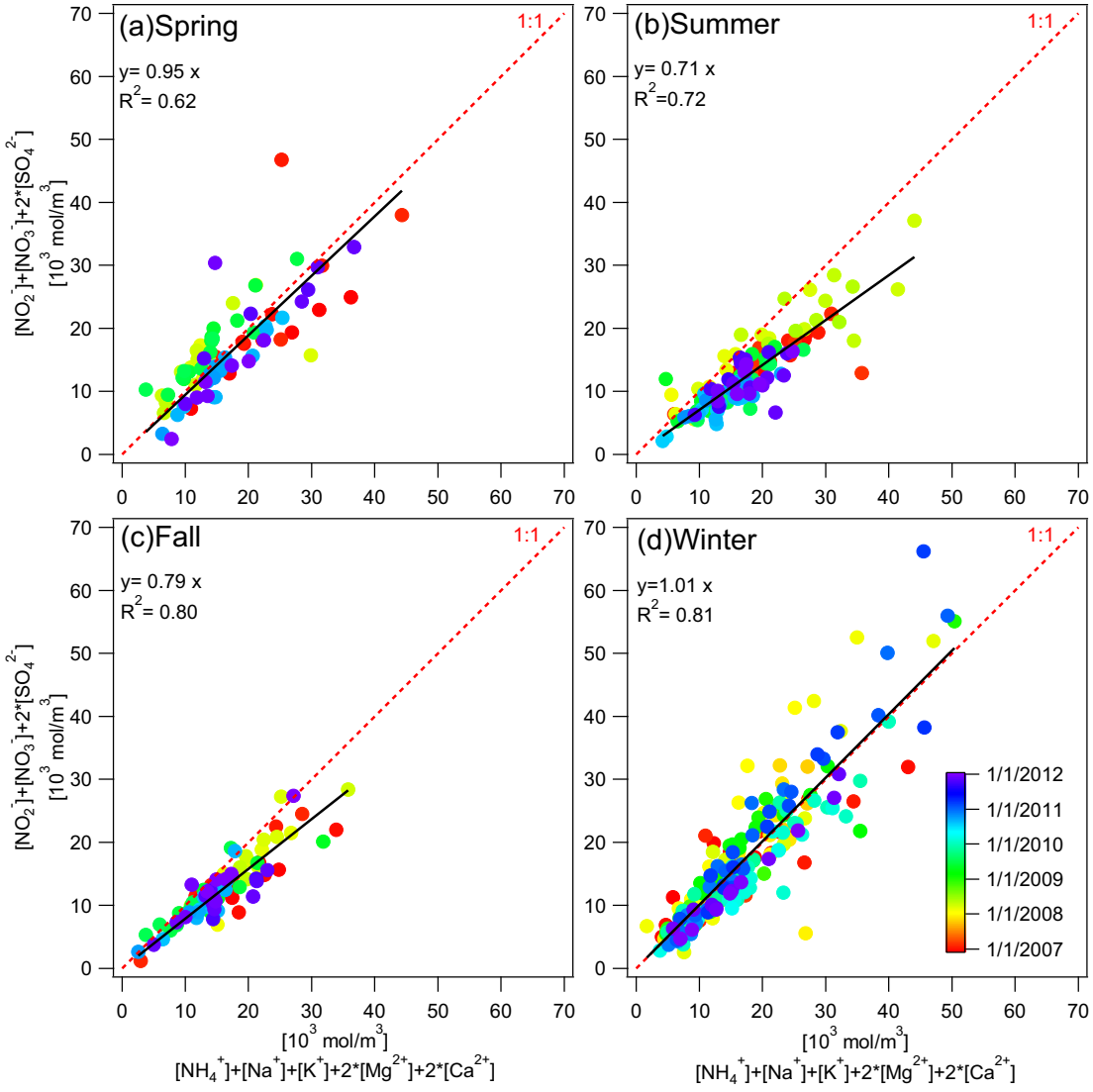

Fig. 9. Seasonal charge balance, where the different colors represent the various sampling periods. (For interpretation of the references to colour in this figure legend, the reader is referred to the web version of this article.)

fine particles. This pattern also appears in some fall and spring samples. This issue can be further evaluated by considering the overall ionic charge balance of measured fine particle anion (NO_2^-, NO_3^-, SO_4^{2-}) and cation (NH_4^+, Na^+, K^+, Mg^{2+}, Ca^{2+}) concentrations. Fig. 9 presents the seasonal variation of the ionic charge balance. During spring and winter, the charge balance is very close to 1:1. During fall and, especially, summer, however, the charge balance generally indicates a deficiency of anions. Previous studies (Barsanti et al., 2009; Trebs et al., 2005) have reported that organic acids such as oxalic acid can be important contributors to the charge balance of fine mode aerosols. The warm season anion deficit observed here is consistent with higher organic acid concentrations during summer, coinciding with periods of enhanced photochemical production of secondary organic aerosols and increased biomass burning. Future measurements of summertime Boulder fine particle concentrations will include analysis of oxalate.

4. Conclusion

A five-year study of concentrations of gaseous NH_3 and HNO_3 and of fine particle inorganic ions was conducted in an active gas production region in Boulder, Wyoming. The five-year annual mean concentrations of NH_3, HNO_3, NH_4^+, NO_3^- and SO_4^{2-} were 0.17, 0.19, 0.26, 0.32, and 0.48 μg m^{-3}, respectively. NH_3 exhibited a strong seasonal variation, with higher concentrations during the summer and lower concentrations during the winter. The low annual average NH_3 mixing ratio of 0.30 ppb suggests that the default value of 1 ppb often used in regional assessments of visibility impacts from NO_x source emissions is higher than necessary.

Observed NH_3 concentrations correlated well with ambient temperature indicating the important influence of temperature on emissions and, likely, the greater long distance transport of those emissions during warmer times of year when mixing layers deepen. By contrast, higher concentrations of particulate NO_3^- were observed in the winter when lower temperatures favor formation of NH_4NO_3. HNO_3 concentrations showed an unusual bimodal seasonal variation with higher levels both in summer (an expected result of active photochemical oxidation and a tendency for NH_4NO_3 to decompose at higher temperatures) and in winter. The unusual winter HNO_3 peak appears to be the result of active photochemical processing of local NO_x emissions in a shallow boundary layer during periods of snow cover and a lack of NH_3 to fully tie up HNO_3 through fine particle NH_4NO_3 formation. Examination of the equilibrium thermodynamics of NH_4NO_3 formation, seasonal local temperatures, and available concentrations of gaseous NH_3 and HNO_3, indicates that NH_4NO_3 should be expected primarily in winter, as observed.

Acknowledgments

The authors thank Amy Sullivan, Xi (Doris) Chen, Katie (Beem) Benedict, Arsineh Hecobian, Yele Sun and Ali (Bote) Willey at Colorado State University for their helpful suggestions and support of the measurement program. The authors also thank Jennifer Frazier of the Wyoming Department of Environmental Quality/Air Quality Division and Ted J. Porwoll of the U.S. Forest Service for carrying out on-site operations.

Appendix A. Supplementary data

Supplementary data related to this article can be found at http://dx.doi.org/10.1016/j.atmosenv.2013.10.007.

References

Adon, M., Galy-Lacaux, C., Yoboué, V., Delon, C., Lacaux, J.P., Castera, P., Gardrat, E., Pienaar, J., Al Ourabi, H., Laouali, D., Diop, B., Sigha-Nkamdjou, L., Akpo, A., Tathy, J.P., Lavenu, F., Mougin, E., 2010. Long term measurements of sulfur dioxide, nitrogen dioxide, ammonia, nitric acid and ozone in Africa using passive samplers. Atmos. Chem. Phys. 10, 7467–7487.

Anderson, N., Strader, R., Davidson, C., 2003. Airborne reduced nitrogen: ammonia emissions from agriculture and other sources. Environ. Int. 29, 277–286.

Andreae, M.O., 1983. Soot carbon and excess fine potassium: long-range transport of combustion-derived aerosols. Science 220, 1148–1151.

Bari, A., Ferraro, V., Wilson, L.R., Luttinger, D., Husain, L., 2003. Measurements of gaseous HONO, HNO_3, SO_2, HCl, NH_3, particulate sulfate and $PM_{2.5}$ in New York, NY. Atmos. Environ. 37, 2825–2835.

Barsanti, K.C., McMurry, P.H., Smith, J.N., 2009. The potential contribution of organic salts to new particle growth. Atmos. Chem. Phys. 9, 2949–2957.

Beem, K.B., Raja, S., Schwandner, F.M., Taylor, C., Lee, T., Sullivan, A.P., Carrico, C.M., McMeeking, G.R., Day, D., Levin, E., Hand, J., Kreidenweis, S.M., Schichtel, B., Malm, W.C., Collett Jr., J.L., 2010. Deposition of reactive nitrogen during the Rocky Mountain Airborne Nitrogen and Sulfur (RoMANS) study. Environ. Pollut. 158, 862–872.

Behera, S.N., Sharma, M., 2010. Investigating the potential role of ammonia in ion chemistry of fine particulate matter formation for an urban environment. Sci. Total Environ. 408, 3569–3575.

Benedict, K.B., Day, D., Schwandner, F.M., Kreidenweis, S.M., Schichtel, B., Malm, W.C., Collett Jr., J.L., 2013. Observations of atmospheric reactive nitrogen species in Rocky Mountain National Park and across northern Colorado. Atmos. Environ. 64, 66–76.

Clarisse, L., Clerbaux, C., Dentener, F., Hurtmans, D., Coheur, P.-F., 2009. Global ammonia distribution derived from infrared satellite observations. Nat. Geosci. 2, 479–483.

Cowell, D.A., Apsimon, H.M., 1998. Cost-effective strategies for the abatement of ammonia emissions from European agriculture. Atmos. Environ. 32, 573–580.

Duan, F., Liu, X., Yu, T., Cachier, H., 2004. Identification and estimate of biomass burning contribution to the urban aerosol organic carbon concentrations in Beijing. Atmos. Environ. 38, 1275–1282.

Edgerton, E.S., Saylor, R.D., Hartsell, B.E., Jansen, J.J., Alan Hansen, D., 2007. Ammonia and ammonium measurements from the southeastern United States. Atmos. Environ. 41, 3339–3351.

Gong, L., Lewicki, R., Griffin, R.J., Flynn, J.H., Lefer, B.L., Tittel, F.K., 2011. Atmospheric ammonia measurements in Houston, TX using an external-cavity quantum cascade laser-based sensor. Atmos. Chem. Phys. Discuss 11, 16335–16368.

Groot Koerkamp, P.W.G., Metz, J.H.M., Uenk, G.H., Phillips, V.R., Holden, M.R., Sneath, R.W., Short, J.L., White, R.P.P., Hartung, J., Seedorf, J., Schröder, M., Linkert, K.H., Pedersen, S., Takai, H., Johnsen, J.O., Wathes, C.M., 1998. Concentrations and emissions of ammonia in livestock buildings in northern Europe. J. Agric. Eng. Res. 70, 79–95.

Gupta, A., Kumar, R., Kumari, K.M., Srivastava, S.S., 2003. Measurement of NO_2, HNO_3, NH_3 and SO_2 and related particulate matter at a rural site in Rampur, India. Atmos. Environ. 37, 4837–4846.

Heald, C.L., Collett, J.L., Lee, T., Benedict, K.B., Schwandner, F.M., Li, Y., Clarisse, L., Hurtmans, D.R., Van Damme, M., Clerbaux, C., Coheur, P.F., Philip, S., Martin, R.V., Pye, H.O.T., 2012. Atmospheric ammonia and particulate inorganic nitrogen over the United States. Atmos. Chem. Phys. 12, 10295–10312.

Hegg, D.A., Radke, L.F., Hobbs, P.V., Riggan, P.J., 1988. Ammonia emissions from biomass burning. Geophys. Res. Lett. 15, 335–337.

Jaffe, D., Hafner, W., Chand, D., Westerling, A., Spracklen, D., 2008. Interannual variations in PM2.5 due to wildfires in the Western United States. Environ. Sci. Technol. 42, 2812–2818.

Lee, H.S., Kang, C.-M., Kang, B.-W., Kim, H.-K., 1999. Seasonal variations of acidic air pollutants in Seoul, South Korea. Atmos. Environ. 33, 3143–3152.

Lee, T., Kreidenweis, S.M., Collett, J.L., 2004. Aerosol ion characteristics during the big bend regional aerosol and visibility observational study. J. Air Waste Manag. Assoc. 54, 585–592.

Lee, T., Yu, X., Ayres, B., Kreidenweis, S., Malm, W., Collett, J.L., 2008. Observations of fine and coarse particle nitrate at several rural locations in the United States. Atmos. Environ. 42, 2720–2732.

Li, Y., Schwab, J.J., Demerjian, K.L., 2006. Measurements of ambient ammonia using a tunable diode laser absorption spectrometer: characteristics of ambient ammonia emissions in an urban area of New York City. J. Geophys. Res. Atmos. 111, D10S02.

Lin, Y., Cheng, M., Ting, W., Yeh, C., 2006. Characteristics of gaseous HNO_2, HNO_3, NH_3 and particulate ammonium nitrate in an urban city of Central Taiwan. Atmos. Environ. 40, 4725–4733.

Malm, W.C., Schichtel, B.A., Pitchford, M.L., Ashbaugh, L.L., Eldred, R.A., 2004. Spatial and monthly trends in speciated fine particle concentration in the United States. J. Geophys. Res. Atmos. 109, D03306.

McMeeking, G.R., Kreidenweis, S.M., Baker, S., Carrico, C.M., Chow, J.C., Collett, J.L., Hao, W.M., Holden, A.S., Kirchstetter, T.W., Malm, W.C., Moosmüller, H., Sullivan, A.P., Wold, C.E., 2009. Emissions of trace gases and aerosols during the open combustion of biomass in the laboratory. J. Geophys. Res. Atmos. 114, D19210.

McMurray, J., Roberts, D., Fenn, M., Geiser, L., Jovan, S., 2013. Using epiphytic lichens to monitor nitrogen deposition near natural gas drilling operations in the wind river Range, WY, USA. Water Air Soil Pollut. 224, 1–14.

Meng, Z.Y., Lin, W.L., Jiang, X.M., Yan, P., Wang, Y., Zhang, Y.M., Jia, X.F., Yu, X.L., 2011. Characteristics of atmospheric ammonia over Beijing, China. Atmos. Chem. Phys. 11, 6139–6151.

Misselbrook, T.H., Van Der Weerden, T.J., Pain, B.F., Jarvis, S.C., Chambers, B.J., Smith, K.A., Phillips, V.R., Demmers, T.G.M., 2000. Ammonia emission factors for UK agriculture. Atmos. Environ. 34, 871–880.

Nowak, J.B., Neuman, J.A., Bahreini, R., Brock, C.A., Middlebrook, A.M., Wollny, A.G., Holloway, J.S., Peischl, J., Ryerson, T.B., Fehsenfeld, F.C., 2010. Airborne observations of ammonia and ammonium nitrate formation over Houston, Texas. J. Geophys. Res. Atmos. 115, D22304.

Plessow, K., Spindler, G., Zimmermann, F., Matschullat, J., 2005. Seasonal variations and interactions of N-containing gases and particles over a coniferous forest, Saxony, Germany. Atmos. Environ. 39, 6995–7007.

Sather, M.E., Mathew, J., Nguyen, N., Lay, J., Golod, G., Vet, R., Cotie, J., Hertel, T., Aaboe, E., Callison, R., Adam, J., Keese, D., Freise, J., Hathcoat, A., Sakizzie, B., King, M., Lee, C., Oliva, S., San Miguel, G., Crow, L., Geasland, F., 2008. Baseline ambient gaseous ammonia concentrations in the Four Corners area and eastern Oklahoma, USA. J. Environ. Monit. 10, 1319–1325.

Schnell, R.C., Oltmans, S.J., Neely, R.R., Endres, M.S., Molenar, J.V., White, A.B., 2009. Rapid photochemical production of ozone at high concentrations in a rural site during winter. Nat. Geosci. 2, 120–122.

Seinfeld, J.H., Pandis, S.N., 2006. Atmospheric Chemistry and Physics: From Air Pollution to Climate Change. Wiley.

Sharma, M., Kishore, S., Tripathi, S.N., Behera, S.N., 2007. Role of atmospheric ammonia in the formation of inorganic secondary particulate matter: a study at Kanpur, India. J. Atmos. Chem. 58, 1–17.

Stelson, A.W., Seinfeld, J.H., 2007. Relative humidity and temperature dependence of the ammonium nitrate dissociation constant. Atmos. Environ. 41 (Suppl.), 126–135.

Sutton, M.A., Dragosits, U., Tang, Y.S., Fowler, D., 2000. Ammonia emissions from non-agricultural sources in the UK. Atmos. Environ. 34, 855–869.

Sutton, M.A., Place, C.J., Eager, M., Fowler, D., Smith, R.I., 1995. Assessment of the magnitude of ammonia emissions in the United Kingdom. Atmos. Environ. 29, 1393–1411.

Trebs, I., Metzger, S., Meixner, F.X., Helas, G., Hoffer, A., Rudich, Y., Falkovich, A.H., Moura, M.A.L., da Silva Jr., R.S., Artaxo, P., Slanina, J., Andreae, M.O., 2005. The NH_4^+–NO_3^-–Cl^-–SO_4^{2-}–H_2O aerosol system and its gas phase precursors at a pasture site in the Amazon Basin: how relevant are mineral cations and soluble organic acids? J. Geophys. Res. Atmos. 110, D07303.

Walker, J.T., Whitall, D.R., Robarge, W., Paerl, H.W., 2004. Ambient ammonia and ammonium aerosol across a region of variable ammonia emission density. Atmos. Environ. 38, 1235–1246.

Yu, X., Lee, T., Ayres, B., Kreidenweis, S., Malm, W., Collett, J.L., 2006. Loss of fine particle ammonium from denuded nylon filters. Atmos. Environ. 40, 4797–4807.